Defect Pattern Analysis of the Alloy Steel Ingotsthrough Scanning Electron Microscopy, Energy Dispersive Spectroscopy and Ultrasonic Test after Forging

Seung-Dai Kim[1]

[1](Department of Mechanical Materials Engineering/ NambuUniversity, Republic of Korea)

ABSTRACT : *In this study, the types and causes of defects found after forging and machining were analyzed for four alloy steel ingots.Forged carbon steel, silico-manganese steel, hardenability chromium molybdenum steel, nickel chromium molybdenum steel, which have undergone casting and heat treatment processes, were used as specimen materials.Ingots were produced through EAF, LF, VD, casting and slow cooling processes.The chemical composition of the alloy steel was analyzed by XRF instrument.The defects of machined ingot specimens were analyzed using ultrasonic test, scanning electron microscopy, energy dispersive spectroscopy, and optical microscopy.The most frequent ingot defect patterns in the four specimens in this study were non-metallic inclusions.As a result of SEM analysis, it seems that the cause of defects in the ingot defect part is a mixed component of the exothermic material and the de-oxidation product inclusions.It seems possible to predict cracks by simultaneously considering the internal crack temperature and strain of the silico-manganese alloy.Since internal cracks in large forgings can shorten product life, it was necessary to consider the influence of critical values of temperature, deformation, and holding time, which are parameter elements.To control inclusions, it was necessary to properly design the overlying slag composition to exhibit a low liquidus temperature and a soft primary phase.Since the inclusion composition gradually changes to the upper layer slag composition over time, the refining time is very important in determining the chemical properties of the inclusion.The results of this experiment can contribute to the establishment of a crack prevention process in the process of free forging large ingots.*
KEYWORDS –*Ingots, Ultrasonic Test, Defect Pattern, Forging, Casting, Inclusions*

I. INTROD1UCTION

When casting alloy steel ingots on a large scale, the analysis of segregation defects in the cast structure is complicated according to the solidification process, and is particularly important when the ingot undergoes plastic deformation.Equiaxialmolten steel emerges as heat escapes from the solid-liquid interface through the mold to the surrounding air.The deposited region of the mold consists of ceramic inclusions that appear in the form of oriented fragments of dendrites that grow as they move towards the axis of the ingot due to the gravitational action of the viscosity gradient. Therefore, Stokes' law is applied to the analysis of sedimentary layers in ingot casting [1].

Non-metallic inclusions in alloy steel are classified into intrinsic and extrinsic inclusions. Intrinsic inclusions are precipitated deoxidation products or inclusions during cooling, such as Al_2O_3 in aluminum-killed steel, SiO_2 in silicon-killed steel. Extrinsic inclusions are formed by the chemical and mechanical interaction of steel with its surroundings, and they are known to have detrimental effects on mechanical properties, usually because of their near-surface location and size. The causes of extrinsic inclusions are lining erosion, chemical reactions and re-oxidation.

When a misch-metal composition is added to molten steel, since RE-sulphides or RE-oxy sulphides are preferentially precipitated and reacted with S, precipitation of MnS can be prevented during solidification.

Defects increase as the ingot size increases, and these defects directly affect the performance of the final product and limit the selection of subsequent heat treatment methods and processes.

Since they have a higher melting point than MnS, their hot deformability is small, and they do not spread in the rolling direction during hot rolling, so they have mechanical properties in the thickness and width directions, particularly ductility, and are not fractured during forging[2-3].

In particular, patterns of casting defects such as macro-segregation, shrinkage cavities, and porosity that inevitably occur in steel ingots due to solute redistribution, time-dependent reduction in solidification rate, and multiphase melt flow during solidification during the casting of large ingots are investigated.

II.   EXPERIMENTAL METHOD

2.1 Chemical Composition Analysis of the Specimens

Table 1 shows the results of analyzing the chemical composition of the ingot specimen material using an EDXRF analyzer(RIGAKU, NEX CG Ⅱ)for the following four alloy steels: Forged carbon steel(FCS), silico-manganese steel(SMS), hardenability chromium molybdenum steel(HCMS), nickel chromium molybdenum steel(NCMS).

Fig. 1 shows the shape of the ingot and the collected specimen before preparing for the slice specimen among the four specimens used in this study.

Table 1. Chemical composition(wt%)

Specimens	Elements							
	C	Si	Mn	P	S	Cr	Ni	Mo
FCS	0.58	0.57	0.41	0.020	0.013	-	-	-
SMS	0.42	0.25	1.02	0.013	0.002	0.13	0.06	-
HCMS	0.19	0.26	0.56	0.018	0.012	0.57	1.75	0.23
NCMS	0.32	0.29	0.67	0.017	0.011	1.56	1.63	0.25

(a) Alloy steel ingot(b) Specimens shape

Figure 1. The sample shape of the previous stage for slice specimen

2.2 Machining of Alloy Steel Ingots

Forging was performed to remove pores, which act as the most fatal defects of thecast structures.Hot open die forging was performed and upsetting and cogging processes were used.

The effective strain was selected as a factor for void closure.The Stress Tri-axiality Based model (STB), the Zhang model, and the CicaPoro model were reviewed as pore closure models[4].

The mill scale removal of the ingot casting was performed by rough machining using a CNC lathe (Doosan) to check cracks or defects on the surface of the casting.

2.3 Defect Patterns Analysis of the Machined Specimens through Inspection Tools

After solidification, the specimens were transversely cut into blocks consisting of 30 cm thick sections of the tower and ingot body for identification.Then, two plates (60 cm × 40 cm × 2.0 cm) were sliced from each side.For each slice, 100 samples (7 cm × 5 cm × 2 cm) were regularly cut.

Optical microscopic analysis was observed after etching the specimen.The defectmorphology of ingots is usually examined by optical microscopy, but scanning electron microscopy (TESCAN, VEGA) was used to identify details because it could not reveal all details of the morphology of some single defects. also, Quantitative analysis spectrum was obtained from energy dispersive spectroscopy[5].

The defects between the voids and cracks in the ingot were investigated by ultrasonic testing (Olympus, EPOCH 650).the differences between ingot voids and cracks were identified by using 2~4 MHz longitudinal and shear transducers and placing them at various angles of incidence and reception.

III.   RESULTS AND DISCUSSION

3.1 Defect Patterns Analysis of the Machined Specimens through Ultrasonic Testing

The results of distinguishing defects between voids and cracks for four types of alloy steel through ultrasonic testing are shown in Fig 2 and Fig. 3.As the incident wave collides with the crack tip, the diffraction

amplitude varies depending on the reception angle.It was found that the shape and size of voids depended on the reception angle of the incident wave scattering and the amplitude of the scattered wave[6].

(a) Indication size: Ø 10.01 mm   (b) Indication size: Ø 8..35 mm
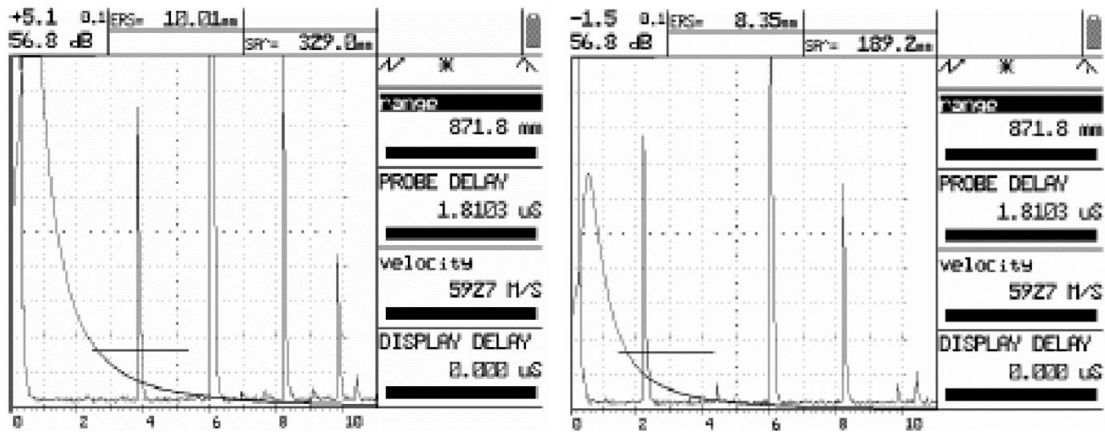
Indication depth: 329.8mm   Indication depth: 189.2 mm

Figure 2. Defects indication pattern by V-type segregation zone in the center of the FCS
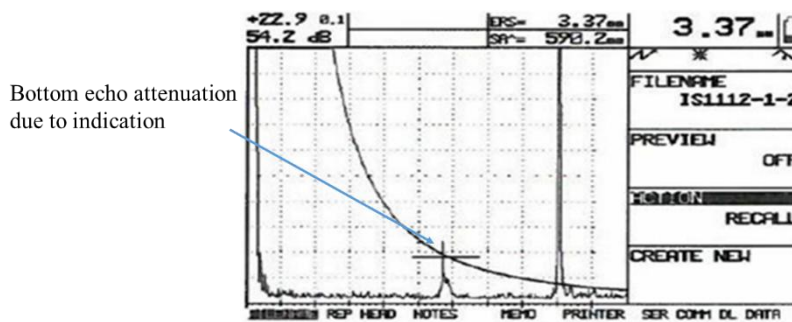
Indication size: Ø 3.37 mm , Indication depth: 590.2 mm

Figure 3. Defect indication pattern by sedimentarycrystallization zone in the FCS
: Inclusion trap pattern

The effect of pressure on the heat transfer boundary condition is considered to be that gravity, buoyancy and drag forces play a key role in the movement behavior of inclusions during the solidification process.

This is consistent with the report that increasing the pressure near the columnar dendrites reduces the inclusion concentration of the ingot and makes the inclusion distribution more uniform because the inclusion trapping ability is weakened[7].

Precise control was required because the low-melting phase, which appears due to the precipitation of the molten phase at the solid-liquid interface of the ingot shaft, promotes cracking by creating cracks and voids during solidification.

3.2 Defect Patterns Analysis of the Machined Specimens through Scanning Electron Microscopy, Energy Dispersive Spectroscopy

The mass balance of components involved in the reaction system between oxides and refractories was required, and the composition change of inclusions could be estimated from the de-oxidation equilibrium and mass balance.It is consistent with the theory that the composition of inclusions is strongly temperature dependent and is influenced by the initial total content of reactants in the de-oxidation system[8-9].

It was found that when the total content of metal and oxygen in the initial state is increased, the dependence on temperature is reduced, making it easier to control the composition during the solidification process.

The SEM images and EDS analysis results of the defect zone of specimen FCS are shown in Fig. 4 and Fig. 5.

Elements	
Al_2O_3	70.2
SiO_2	33.8
CaO	1.60
MgO	4.6
Na_2O	2.50
Elements	
Al_2O_3	100

(a) SEM image(150×)	(b) EDS spectrum	(c) Quantitative analysis (wt%)
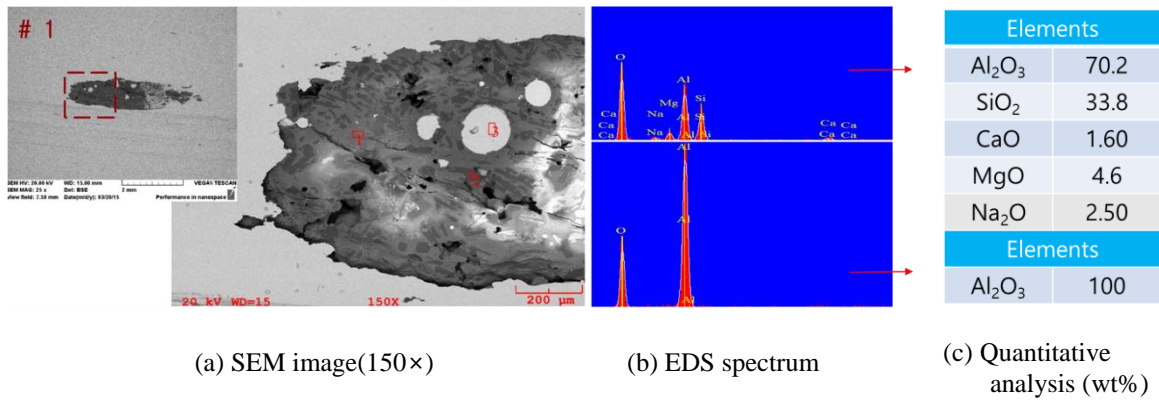
Figure 4. SEM image and EDS analysis of the flaws on FCS #1

Elements	
Al_2O_3	19.7
SiO_2	57.8
TiO	1.50
MnO	21.0
Elements	
SiO_2	100

(a) SEM image(500×)	(b) EDS spectrum	(c) Quantitative analysis (wt%)
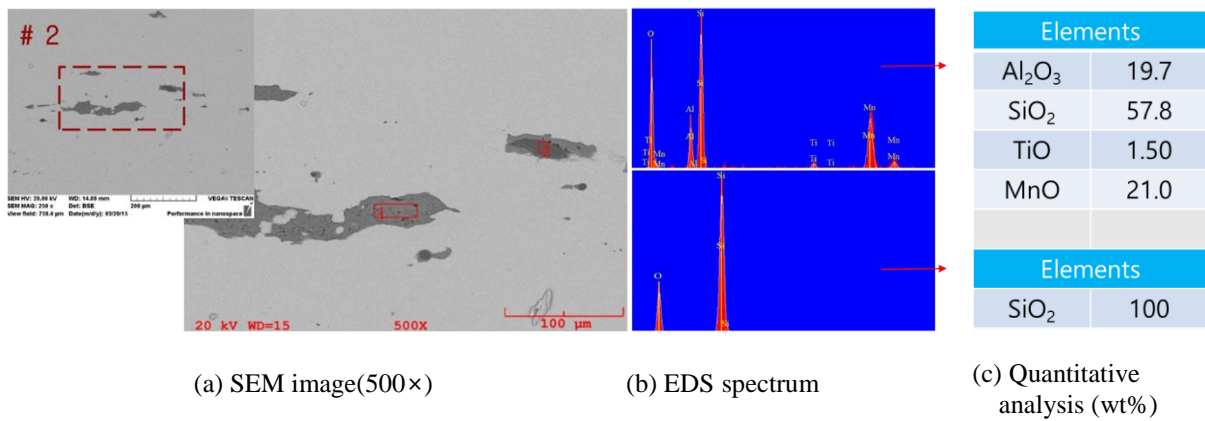
Figure 5. SEM image and EDS analysis of the flaws on FCS #2

The size distribution, composition and capture location were selected for the source of the macro-inclusions on the sample surface.

Ceramic particles should not be present in the ingot in the sedimentary zone of the ingot, and the higher the sedimentary cone, the higher the possibility of unwanted negative macroscopic segregation.

Fig. 6 shows the scanning electron microscopy image and energy dispersive spectroscopy analysis results for defects in specimen SMS.

The non-sulphide macro-inclusions observed were present in the ingot and the size distribution increased as the size decreased.The inclusions are uniformly distributed within the horizontal section of the ingot, but more numerous towards the bottom[10].

Elements	
Al_2O_3	64.4
SiO_2	23.0
CaO	1.20
MgO	11.4
Elements	
Al_2O_3	64.4
SiO_2	23.0
CaO	1.20
MgO	11.4
MnO	2.80
Elements	
Al_2O_3	56.1
SiO_2	32.0
CaO	6.60
MgO	3.80
MnO	1.50

(a) SEM image   (b) EDS spectrum   (c) Quantitative Analysis (wt%)
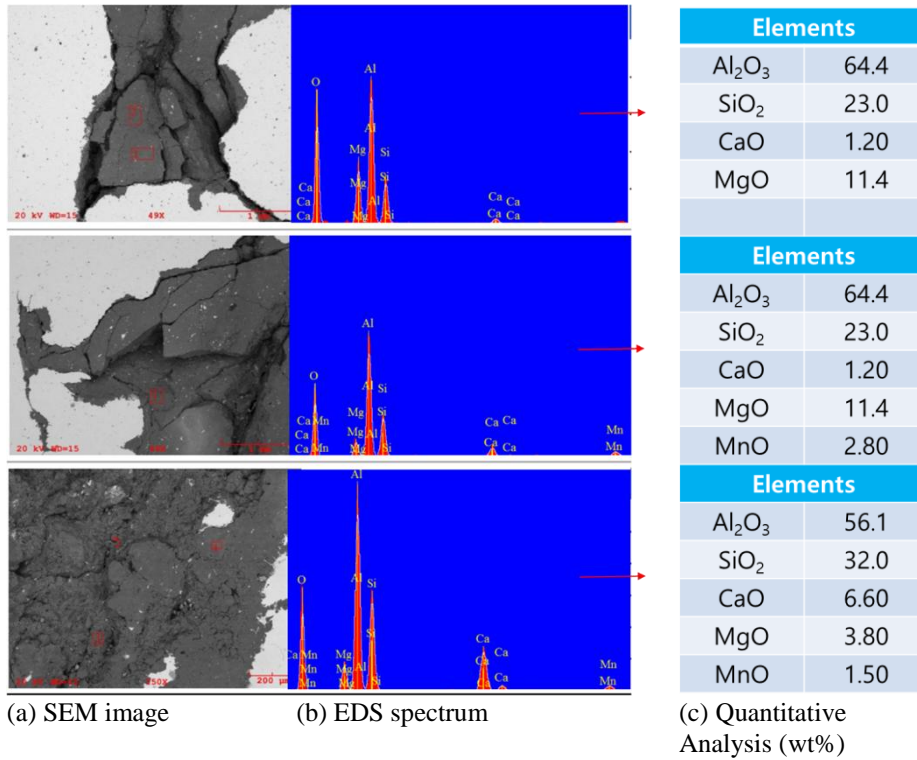
Figure 6. SEM image and EDS analysis of the flaws on SMS
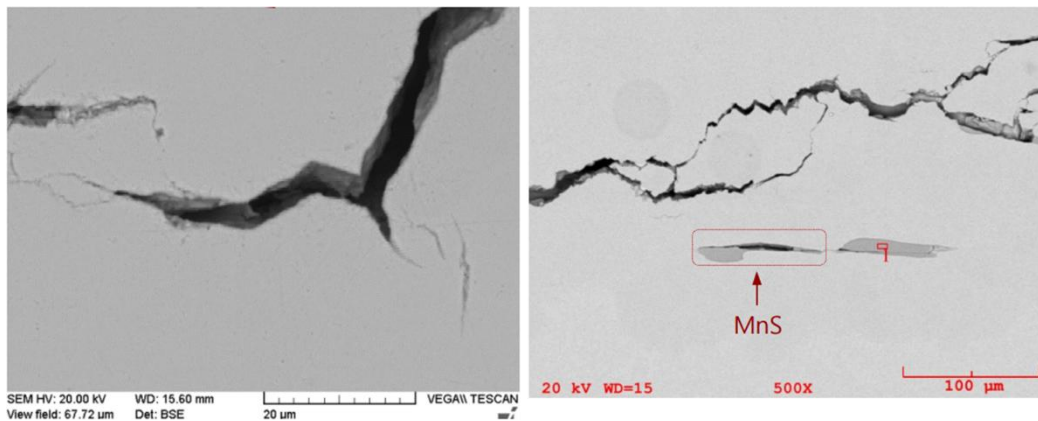
(a) Crack zone   (b) MnS voids morphology of the crack zone

(500×)

Figure 7. SEM imagesof the crack fracture zone on NCMS after forging

Ingot inclusions presumed to be eroded refractories in the ladle block and the nozzle inside the ladle accounted for most of the inclusions.

Fig. 7 shows the SEM image of the crack fracture identified in the specimen NCMS after forging. A crack observed in the forging ingot as the result of increased amount of the sulphur source.

Macro-surface cracks and sub-surface micro-cracks were analyzed as being caused by non-metallic inclusions of alumina and oxide types.

The cause of the inclusions was consistent with the reports of refractory linings, furnace hot-tops and ladle[11].

Micro-cracks appear to be accompanied during the solidification process by carbides existing between the columnar structures of the ingot.

The all segregation defects can promote some cracks in the final product obtained by the forging.
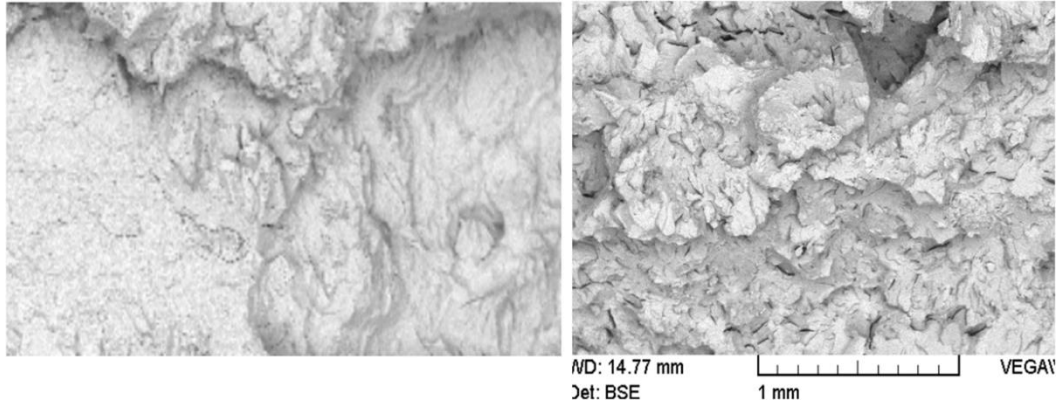
(a) forged crack surface (b) forced fracture surface

Figure 8. Surface morphology difference of the forged crack and forced fracture surface on NCMS
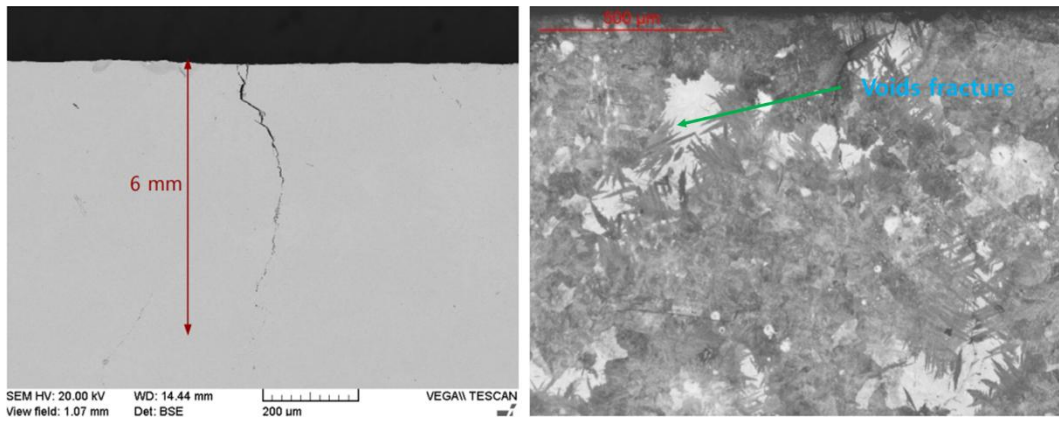
(a) Vertical crack depth from surface(b) Voids fracture image against crack direction

Figure 9. Crack pattern along withembrittlementband structure of the NCMS after forging

Strain criteria of the loss of cohesion can be expressed as equation (1)

$$\Psi_s = \int_0^{\bar{\varepsilon}_f} \frac{d\bar{\varepsilon}}{\bar{\varepsilon}_k (T_\sigma)} \leq 1 \quad (1)$$

Where $\bar{\varepsilon}_k (T_\sigma)$ is the function of workability threshold, $T_\sigma = \frac{\sigma_m}{\bar{\sigma}}$ is the stress tri-axiality, $\bar{\varepsilon}$ is the effective strain, $\bar{\sigma}$ is the effective stress, $\bar{\varepsilon}_f$ is the effective strain of fracture and σ_m is the mean stress.

The deformation damage factor is given by Equation (2).

$$\Psi_s = \left[\frac{(\bar{\varepsilon}_{ij})_1 + (\Delta\bar{\varepsilon}_{ij})_2}{\bar{\varepsilon}_k(T_\sigma)_{ij}} \right]^t \leq 1 \quad (2)$$

where *t* is micro-crack healing coefficient

Equation 2 describes the 'healing' of micro-cracks as cracks start and increase during plastic deformation, and the process of bonding cracks under tri-axial compression conditions[12].
It was necessary to apply the deformation criterion of loss of cohesion to predict defect-based cracking of forged ingots.

3.3 Defect Patterns Analysis of the Machined Specimens by the Optical Microscopy

In silico-manganese steel (SMS), $\Phi 4$ inclusions caused by exothermic source + de-oxidation products were confirmed on the indicator.

The main components of the inclusion were Al_2O_3 and SiO_2, and it was confirmed that an inclusion trap was formed in the bottom solidification part due to the endothermic reaction of the exothermic material including Fe_2O_3, TiO_2, CaO, MgO and Na_2O[13].
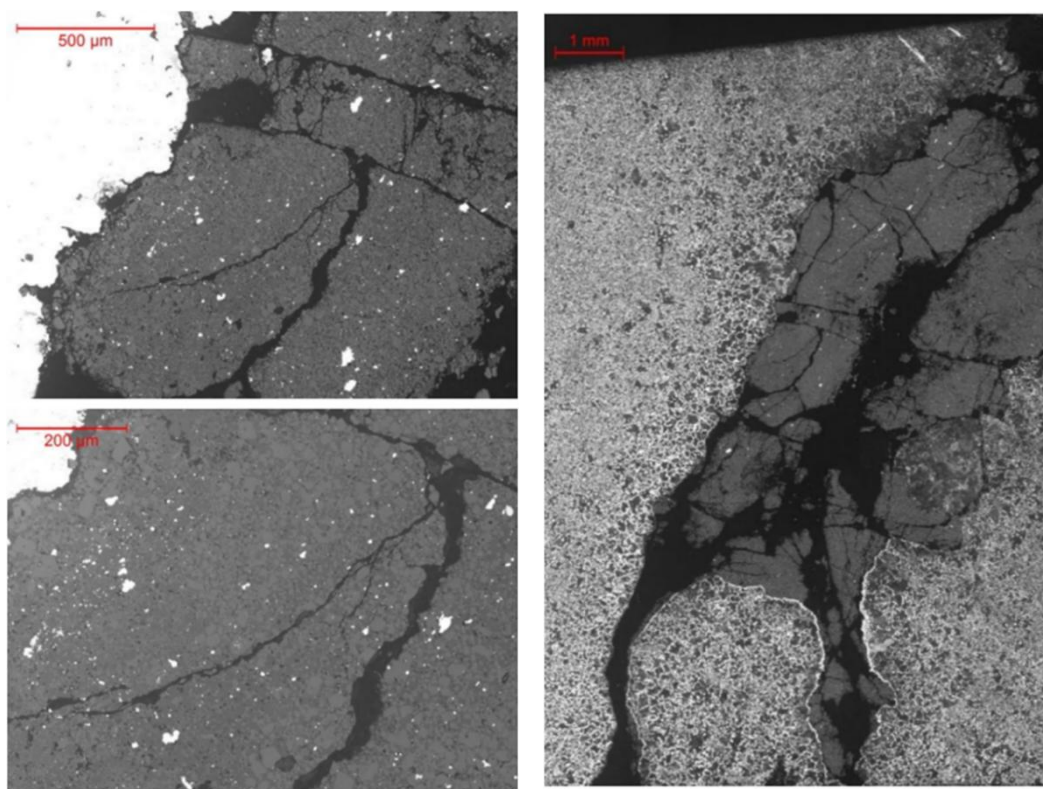
(a) Crack due to little inclusion zone   (b) Crack due to massive inclusion zone

Figure 10. Crack zone image of SMS surface by the optical microscope after forging

As for void closure, the two most important parameters were void shape and load direction relative to void orientation.

The result of observing the crack zone image on the surface of the specimen SMS by an optical microscope after forging is shown in Fig. 10.

It is considered according to the report that it is important to control the hydrogen content of the casting to less than 6 ppm to prevent the occurrence of pinholes in alloy steel.

Hydrogen trapping is created during the melting process and has been known to be a problem with alloys containing nickel in castings and at low temperatures.

Hydrogen trapping or Mns inclusions cause serious problems in the process of processing or using alloy steel ingots, so they must be strictly controlled.

Precipitates of carbide trapped between the dendrite branches are known to promote the propagation of some cracks during ingot forging.

It is known that the presence of inclusions such as ceramic particles in the deposition zone of the ingot increases the probability of cracking during solidification due to negative macroscopic segregation[14].

It can be appearing significant segregation defects during the thermophoresis. So,

Large sized carbides forming macro-bands may have the same crack origin as the "A" or "V" type macro-segregation effect.

The more micro-segregation accompanying the deposition of some equiaxed grains on the surface of the sedimentary cone, the more likely it is to cause A-type macro-segregation.

IV.   CONCLUSION

Patterns of solidification defects such as inclusions, porosity, shrinkage, and macro-segregation that occur during the manufacture of large steel ingots and their formation mechanisms were examined.In the process of post-processing after casting large steel ingots, the main source of crack defects was non-metallic inclusions.

The free crystals emitted from the top and sides of the ingot and the local growth of crystals due to heat transfer generated equiaxial crystal regions at the bottom of the ingot.

The formation of inclusions floating on the top of the ingot seems to be caused by a phenomenon that comes down to the bottom by natural convection and is trapped in the mercy zone.

The source of cracks after machining seems to have been caused by direct hydrogen in the A segregation zone slightly out of the center of the ingot.

In the top part of the ingot, positive segregation was formed, and in the center of the ingot, a V segregation zone appeared. According to the ultrasonic flaw detection, the defect occurred in the V segregation zone was Porosity, Porosity in the V segregation zone led to defects due to lack of forging ratio after forging.

Cracks were generated along the brittle band structure in MnS around the cracks, and these defects are considered to be caused by hydrogen.

In order to obtain defect-free alloy steel ingots after forging large ingots, the relationship between anvil shape, hydrostatic pressure, and effective strain, which affect pore compression and pore defect removal, will be studied in the future.

REFERENCES

[1]   W. Wołczyńskia, P. Kwapisińskib, B. Kaniaa, W. Wajdaa, W. Skuzaa and A.W. Bydałekc, Numerical Model for Solidification Zones Selection in the Large Ingots. Archives of Foundry Engineering,15(4),2015, 87-90. DOI: 10.1515/afe-2015-0085
[2]   X. X. Zhang, Z. S. Cui, W. Chen andY. Li, A criterion for void closure in large ingots during hot forging. Journal of Materials Processing Technology, 209(4), 2009, 1950-1959.DOI: 10.1016/j.jmatprotec.2008.04.051
[3]   J. Fruhstorfer, L. Schöttler, S. Dudczig, G. Schmidt, P. Gehre andC. G.Aneziris, Erosion and corrosion of alumina refractory by ingot casting steels. Journal of the European Ceramic Society, 36(5),2016, 1299-1306.DOI: 10.1016/j.jeurceramsoc.2015.11.038
[4]   Y. Liu, Z. Zhang, G. Li, Q. Wang and B. Li, Effect of current on segregation and inclusions characteristics of dual alloy ingot processed by electroslagremelting. High Temperature Materials and Processes, 38, 2019, 207-218. DOI: 10.1515/htmp-2017-0144
[5]   F. D. Marillia, M. Jahazi, S. Lafreniere and P. Belanger, Design and Optimisation of a phased array transducer for ultrasonic inspection of large forged steel ingots. NDT & E International, 103, 2019,119-129.DOI: 10.1016/j.ndteint.2019.02.007
[6]   K Chen, Y Yang, G Shao and K Liu, Strain function analysis method for void closure in the forging process of the large-sized steel ingot. Computational Materials Science, 51(1), 2012, 72-77.DOI: 10.1016/j.commatsci.2011.07.011
[7]   G. Lesoult, Macrosegregation in steel strands and ingots: Characterisation, formation and consequences. Materials Science and Engineering: A, 413-414(15), 2005, 19-29. DOI: 10.1016/j.msea.2005.08.203
[8]   L. Zhang, B. Rietow, B. G. Thomas and K. Eakin, Large inclusions in plain-carbon steel ingots cast by bottom teeming. ISIJ international, 46(5), 2006, 670-679.DOI: 10.2355/isijinternational.46.670
[9]   M. Bitterlin, A.Loucif, N.Charbonnier, M.Jahazi, L. P.Lapierre-Boire, and J, B. Morin, Cracking mechanisms in large size ingots of high nickel content low alloyed steel. Engineering Failure Analysis, 68, 2016, 122-131.DOI: 10.1016/j.engfailanal.2016.05.027
[10]   C. Zhang, A.Loucif, M.Jahazi, R. Tremblay and L. P.Lapierre, On the effect of filling rate on positive macrosegregation patterns in large size cast steel ingots. Applied Sciences, 8(10), 12018, 878.DOI: 10.3390/app8101878
[11]   M. Jamil, A. M. Khan, H. Hegab, S. Sarfraz, N. Sharma, M. Mia and C. I. Pruncu, Internal cracks and non-metallic inclusions as root causes of casting failure in sugar mill roller shafts. Materials, 12(15), 2019, 2474.DOI: 10.3390/ma12152474
[12]   M. Kukuryk, Analysis of deformation and prediction of cracks in the cogging process for die steel at elevated temperatures. Materials, 13(24), 2020, 5589.DOI: 10.3390/ma13245589
[13]   J. Li, X.W. Xu, N. Ren, M. X. Xia andJ. G. Li, A review on prediction of casting defects in steel ingots: from macrosegregation to multi-defect model. Journal of Iron and Steel Research International, 29, 2022, 1-14.DOI: 10.1007/s42243-022-00848-7
[14]   M.Wu, A. Ludwig andA. Kharicha, four phase model for the macrosegregation and shrinkage cavity during solidification of steel ingot. Applied mathematical modelling, 41, 2017, 102-120. DOI: 10.1016/j.apm.2016.08.023